Paper

Lupus
0(0) 1–10

DOI: 10.1177/0961203320929746
journals.sagepub.com/home/lup
SAGE

Effect of indole-3-carbinol on transcriptional profiling of wound-healing genes in macrophages of systemic lupus erythematosus patients: an RNA sequencing assay

Farnaz Eghbalpour[1], Mehrdad Aghaei[2], Mansour Ebrahimi[3,4], Mohammad Reza Tahsili[4], Masoud Golalipour[5], Saeed Mohammadi[6] and Yaghoub Yazdani[6,7]

Abstract

Background: Relapses and flares with delayed wound healing are among the main symptoms of systemic lupus erythematosus (SLE), a rheumatic autoimmune disease. The orientation of immune responses in SLE disease depends on the function of the population of macrophages. This study investigated the effect of indole-3-carbinol (I3C) on transcriptional profiling of macrophage-derived monocytes (MDMs) in four stages of the wound-healing process.

Methods: In the first phase of study, MDMs were generated from peripheral blood mononuclear cells of three new SLE cases (unmedicated) and two healthy controls. The cases and controls were then divided into I3C treated and untreated groups after 24 hours of exposure to I3C. Single-end RNA sequencing was performed using an Illumina NextSeq 500 platform. After comprehensive analysis among differentially expressed genes, *CDKN1A*, *FN1* and *MMP15* were validated by quantitative real-time polymerase chain reaction as upregulated ranked genes involved in wound-healing stages.

Results: The RNA sequencing analysis of treated cases and treated controls versus untreated cases and untreated controls (group 3 vs. group 4) revealed upregulation of various genes, for example: *C1S*, *C1R*, *IGKV1-5*, *IGKV4-1*, *SERPING1*, *IGLC1* and *IGLC2* in coagulation; *ADAM19*, *CEACAM1* and *CEACAM8* in M2 reprogramming; *IRS1*, *FN1*, *THBS1* and *LIMS2* in extracellular matrix organization; and *STAT1*, *THBS1* and *ATP2A3* in the proliferation stage of wound healing.

Conclusions: The results showed that treatment with I3C could modulate the gene expression involved in wound healing in SLE cases and healthy controls.

Keywords
Indole-3-carbinol, SLE, RNA-seq, MDMs

Date received: 29 February 2020; accepted: 5 May 2020

Introduction

The body is ready to heal itself at any time, but if the healing process is slowed down, it means that there is a problem. The wound-healing cascade is divided into four overlapping stages: haemostasis, inflammatory, proliferative and remodelling.[1] Deregulation of any of these steps leads to impaired healing. Macrophages are one of the most effective immune cells in various autoimmune diseases, including systemic lupus erythematosus (SLE).[2] Macrophages can play a unique role in

[1]Department of Molecular Medicine, School of Advanced Technologies in Medicine, Golestan University of Medical Sciences, Iran
[2]Golestan Rheumatology Research Centre, Golestan University of Medical Sciences, Iran
[3]School of Agriculture and Veterinary Sciences, University of Adelaide, Australia
[4]School of Basic Sciences, University of Qom, Iran
[5]Medical Cellular and Molecular Research Centre, Golestan University of Medical Sciences, Iran
[6]Stem Cell Research Centre, Golestan University of Medical Sciences, Iran
[7]Infectious Diseases Research Centre, Golestan University of Medical Sciences, Iran

Corresponding author:
Yaghoub Yazdani, Golestan University of Medical Sciences Hezarjarib AV, Gorgan, Iran Gorgan, Golestan 4917937813, Islamic Republic of Iran.
Email: Yazdani@goums.ac.ir

repairing and remodelling wounds, which is why these cells can change their function, though this process is not well understood.[3] At the proliferative stage, angiogenesis should occur to supply oxygen and nutrients required for collagen deposition, tissue formation and epithelialization.

Studies have shown that some environmental factors and endogenous molecules affect the fate of macrophage cells and the development of autoimmune diseases, including SLE, via the molecular pathway of the aryl hydrocarbon receptor (AhR).[4–6]

Using new biological molecules in diagnosis and therapy is one of the most challenging and critical aspects in molecular medicine.[7,8] AhR is a ligand-activated transcription factor and pioneer member of the basic helix–loop–helix-PER-ARNT-SIM family. The AhR–ARNT dimer then binds to upstream regulatory regions of its target genes and leads to chromatin structural configuration through histone acetyltransferase and methyltransferase activities.[9] Eventually, cell transcriptome profiling and epigenetic mechanisms could be changed through canonical (genome-associated) cross-talk between activated AhR and interaction with several signalling pathways (e.g. nuclear factor kappa B, oestrogen receptor and KLF6).[10–12] In non-Xenobiotic Response Element (XRE) or (indirect) activation of AhR, the most stated endogenous ligands such as indole-3-carbinol (I3C), a nutritional supplement, could be found in brassica vegetables might be led to the production of anti-inflammatory cytokines. Today, it has been convincingly documented that disrupted transcription factor networks and gene expression profiles in immune cells contribute to the pro-inflammatory phenotype in SLE.[13] We hypothesized that I3C might be used to change macrophage behaviour through activation of anti-inflammatory pathways in the macrophage-derived monocytes (MDMs) of patients with SLE in order to accelerate wound healing. This study focused particularly on investigating the effect of I3C on remodelling pathway gene expression in MDMs from patients with SLE in order to control the behaviour of macrophages and to promote the wound-healing process and tissue remodelling.[14,15]

To the best of the authors' knowledge, this is the first report to assess the transcriptome profiling of MDMs from SLE patients after treatment with I3C. Accordingly, RNA sequencing (RNA-seq) was performed to identify in vitro gene expression signatures of reprogrammed MDMs with I3C stimuli.[1,16]

Methods

Ethical issues

Approval for this study was provided by the Ethics Committee of Golestan University of Medical Sciences, Gorgan, Iran (project reference number IR.GOUMS.REC.1395.245).

Patients and healthy controls

A total of 15 female patients with SLE, including three newly diagnosed patients in the first phase and 12 new SLE cases in the third phase, were enrolled in this study. All newly diagnosed SLE cases fulfilled at least four of the American College of Rheumatology[17] diagnostic criteria 2014 for SLE.[18–20] None of the new SLE cases had received anti-inflammatory drugs within the six months preceding blood draws. Female healthy controls >18 years old with no history of inflammatory diseases and vaccination within at least six months were also recruited for blood donation. The immunological information of all patients is summarized in Table 1.

Study phase 1

MDM generation and treatment by I3C. Peripheral whole blood (15 mL) was obtained by venipuncture from new SLE cases and healthy controls. Peripheral blood mononuclear cells were purified from fresh buffy coats using a Ficoll density gradient (Baharafshan, Tehran, Iran). Monocytes were enriched with a magnetic cell sorting (MACS) monocyte isolation kit (Miltenyi Biotec, Bergisch Gladbach, Germany).[21] Purified $CD14^+$ cells were allowed to attach to plastic for two to four hours in the incubator and then were differentiated in vitro in RPMI-1640 (Gibco; Life Technologies, Carlsbad, CA) culture medium supplemented with 10% heat-inactivated fetal bovine serum (Gibco; Life Technologies), 10% autologous plasma and 1% penicillin/streptomycin (Gibco; Life Technologies) for six days at 37°C in 5% CO_2. After six days, the monocytes were transformed from a round shape to a fibroblastic-like morphology with pseudopods, and adhesion shapes were observed in the cultured cells. Differentiated MDMs were treated with I3C at a concentration of 10 ng/μL for 24 hours according to a previous study.[22]

Investigation of the effect of I3C on AhR target genes. Among the genes with filtration criteria (fold change ≥ 2 and $p \leq 0.05$), the expression level of two AhR target genes, *CYP1A1* and *CYP1B1*, was validated in five healthy controls and five new SLE cases by quantitative real-time polymerase chain reaction (qRT-PCR).

Study phase 2

Library construction and RNA-seq. Total RNA from MDMs was separately isolated using a RNeasy Mini Kit (Qiagen, Hilden, Germany) according to the

Table 1. Clinical and laboratory characteristics of the patients with SLE in the study.

Phase of study	Subject	CRP (mg/L)	RF	WBC (K/cmm)	ANA (IU/mL)	Anti-dsDNA (IU/mL)	Clinical manifestations
1 and 3	New case 1*	Neg.	Neg.	2200	2.9	619	Leucopaenia, anaemia, arthritis
1 and 3	New case 2*	Neg.	Neg.	4400	2.8	450	Cutaneous anaemia
3	New case 3*	Neg.	Neg.	6300	3200	362	Cutaneous arthritis
3	New case 4	Neg.	Neg.	5500	3.25	35	Cutaneous ulcers
3	New case 5	Neg.	Neg.	6200	4.1	28	Oedema
3	New case 6	1.32	Neg.	7600	2.57	63.9	Arthritis
3	New case 7	Neg.	1+	4600	2.7	41	Cutaneous arthritis
3	New case 8	5.89	3+	4100	>100	23	Cutaneous arthritis
3	New case 9	1.28	2+	3000	2.95	7.9	Arthritis
3	New case 10	2.4	Neg.	3200	210	9.5	Arthritis
3	New case 11	Neg.	Neg.	2700	42.9	8.9	Cutaneous oedema
3	New case 12	Neg.	Neg.	4600	224.9	5.6	Anaemia, arthritis
3	New case 13	0.4	2+	3100	8.3	22.6	Cutaneous arthritis
3	New case 14	Neg.	Neg.	6000	176.5	391	Arthritis
3	New case 15	2.5	1+	3200	146	354	Cutaneous oedema

*Used for RNA sequencing.
RF: rheumatoid factor; WBC: white blood cell.

manufacturer's instructions. Generation of RNA-seq libraries was performed using 1000 ng total RNA according to the manufacturer's instructions for the SureSelect Strand-Specific RNA Library Preparation kits for the Illumina multiplex sample preparation kit. The libraries were sequenced on an Illumina NextSeq 500 (Illumina, San Diego, CA), running control software v2.2.0 (using default parameters) to generate 100 bp single-end reads. Illumina adapters as well as poly (A) or poly (T) sequences were eliminated following pre-processing process.

Data preprocessing and bioinformatics analysis. High-throughput RNA-seq was performed for 10 RNA samples (two treated controls, two untreated controls, three treated cases and three untreated cases) using an Illumina NextGENe Analyzer to explore the effect of I3C on the gene expression of MDMs. Quality control (QC) was performed using a CLC Genomics Workbench based on the QC report to remove any low-quality reads as well as 3′ and 5′ end trimming (www.bioinformatics.babraham.ac.uk/projects/fastqc/). A threshold of $\geq$0.2 reads per kilobase of transcript for million mapped reads (RPKM) was used to identify differentially expressed genes (DEGs) of treated controls versus untreated controls along with treated cases versus untreated cases.[23]

Study groups. In the second phase of the study, four groups were constructed based on CLC Genomics Workbench output results for comparing DEGs of MDMs between cases and controls as well as I3C-treated and untreated groups. Specifically, the groups were: treated controls versus untreated controls (group 1), treated cases versus untreated cases (group 2), treated cases versus treated controls (group 3) and untreated cases versus untreated controls (group 4). Likewise, to create an overview of differentially expressed profiles from the samples used in this work, a fold-change cut-off threshold (log2 fold change $\geq$2 or ≤ -2) and p-value of $\leq$0.05 were applied to define the DEGs.

Gene ontology and pathway analysis. There are several methods to analyse high-throughput biological data. In the present study, genes passing the normalization and filtering (Bonferroni-corrected chi-square $p \leq 0.05$ and fold change $\geq$2 or ≤ -2) were subjected to gene ontology (GO) clustering and pathway analysis. GO clustering was performed using the free online Reactome bioinformatics resource (https://reactome.org/).[24]

Study phase 3

Validation of ranked genes involved in wound healing by qRT-PCR. In the third phase of study, based on DEGs of four different groups, three ranked genes involved in the wound-healing process were selected for qRT-PCR validation. For 15 newly diagnosed SLE cases, three genes (*FN1*, *CDKN1A* and *MMP15*) were validated by qRT-PCR. The primers for qRT-PCR are listed in Table 2.

Table 2. Primer sequences for qRT-PCR gene expression analysis.

Primer name	Gene Bank accession no.	Primer sequence	Amplicon size (bp)	Annealing temperature	Ref.
GAPDH	NM_001256799	F:5′-ACAACTTTGGTATCGTGGAAGG-3′ R:5′-GCCATCACGCCACAGTTTC-3′	101	60	33
CDKN1A	NM_012127	F: 5′-GTGAAAACAGAGCGAGAGAGATG-3′ R:5′-CAGGGGTACAGTGCTAAAGGC-3′	107	61	34
MMP15	NM_002428	F:5'- GTGCTCGACGAAGAGACCAAG-3′ R:5′-TTTCACTCGTACCCCGAACTG-3′	78	61	35
FN1	NM_212482	F:5-CGGTGGCTGTCAGTCAAAG-3′ R:5′-AAACCTCGGCTTCCTCCATAA-3′	130	60	36

qRT-PCR: quantitative real-time polymerase chain reaction; *GAPDH*: glyceraldehyde-3-phosphate dehydrogenase; *CDKN1A*: cyclin-dependent kinase inhibitor 1; *MMP15*: matrix metalloproteinase 15; *FN1*: fibronectin 1.

Results

MDM differentiation

Isolated monocytes with MACS MicroBeads negative selection and >95% purity were cultured with autologous plasma to differentiate into macrophages for six days. M1 and M2 macrophages represent $CD86^+$ and $CD163^+$, respectively, during the reprogramming procedure. The generation of MDMs with the applied protocol was approved via flow cytometry, in which the expression of $CD68^+$, $CD86^+$ and $CD163^+$ was assessed ($CD68^+$: 86.6%; $CD86^+$: 48.6%; $CD163^+$: 44.8%) in monocyte and macrophage gates six days post culture. Once the monocytes fulfilled the morphological characteristics of macrophages, I3C treatment was performed for 24 hours.

AhR target genes

The induction of AhR battery genes by I3C behaved in macrophages as predicted.[22] Thus, high induction of AhR battery genes *CYP1A1* (3.75-fold) and *CYP1B1* (2.41-fold; Supplemental Figure S1) suggested the successful stimulation of AhR signalling by I3C.[25]

RNA-seq

Deep RNA-seq of I3C-treated and untreated monocyte-derived macrophages from two treated controls, two untreated controls, two treated cases and three untreated cases (N=9) with approximately 15 million reads per sample were successfully performed. A total of 154,216,313 sequences and 8,408,974,837 nucleotides were sequenced in all data sets. Almost 96% of the total reads of all the samples passed the 30 Phred score. Mapping stringency was set at 50% of read length mapping at 80% identity. A summary of the statistics of single-end 100 bp clean reads and the average length obtained per sample are listed in Table 3.

The data sets were deposited in the Harvard Dataverse online data repository (https://dataverse.harvard.edu/dataset.xhtml?persistentId=doi:10.7910/DVN/CAEDRI).[26]

GO enrichment analysis

From the CLC software analysis, 58,174 DEGs were identified among all samples. According to the study's goal of elucidating the effect of I3C on approved genes involved in wound healing (available online on www.informatics.jax.org/vocab/gene_ontology/GO:0042060), genes of data sets with a fold change ≥ 2 or ≤ -2 and p-value of ≤ 0.05 were investigated, and finally DEGs of all groups were submitted to the Reactome database. Pathway analysis showed I3C treatment shifted the mRNA profile of MDMs from inflammatory pathways to anti-inflammatory pathways, as *AHR*, *ARNT*, *CYP1A1*, *CYP1B1* and *AHRR* expression was preferably upregulated in the I3C-treated population.

Investigation of the effect of I3C on the gene expression profile of healthy controls

Treatment with I3C was found to modulate different genes in two healthy controls. Among DEGs, 435 genes were upregulated and 1386 genes were downregulated in treated controls compared to untreated controls (group 1). *FN1*, *HMOX1*, *HBEGF*, *FGFR3*, *TLR9*, *GDF15*, *GDF15*, *SNAI1*, *PGF*, *GADD45A*, *COL6A1*, *FAIM2*, *MAPK8IP3* and *CTSF* were identified as upregulated genes involved in different stages of the wound-healing process in group 1.

Table 3. Raw reads statistics of all samples.

Sample ID	Sample RNA-seq ID	Number of reads after trimming	Reads mapped	Average length after trimming	Reads uniquely mapped	Protein coding %	Intron	Total exon
TCA	RNA008_S4_L001_R1_001	17,338,796	17,125,400	75.3	15,340,882	86.72	436,530	14,904,352
TCA	RNA0012_S4_L001_R1_001	15,360,621	14,860,900	74.2	13,426,026	89.05	291,782	13,134,244
TCA	RNA0029_1_S4_L001_R1_001	3,831,277	3,520,022	74.0	3,016,351	83.74	176,479	2,839,872
UCA	RNA009_S4_L001_R1_001	15,879,294	15,707,942	75.4	14,057,823	86.21	729,659	13,328,164
UCA	RNA0013_S4_L001_R1_001	16,867,944	16,537,090	75.2	14,577,167	88.63	350,482	14,226,685
UCA	RNA0026_S4_L001_R1_001	15,320,168	14,379,678	75.3	12,163,402	82.65	1,740,777	10,422,625
TCO	RNA0014_S4_L001_R1_001	24,867,527	24,615,753	75.4	21,616,317	87.23	499,541	21,116,776
TCO	RNA0016_S4_L001_R1_001	15,741,575	15,555,689	75.3	15,555,689	87.67	254,559	13,422,952
UCO	RNA0017_S4_L001_R1_001	16,453,555	16,280,140	75.4	14,187,736	86.48	506,426	13,681,310
UCO	NA0028_S4_L001_R1_001	12,555,556	12,420,322	75.5	10,894,310	84.35	423,374	10,470,936

TCA: treated case; UCA: untreated case; TCO: treated control; UCO: untreated control.

Investigation of the effect of I3C on the gene expression profile of SLE cases

In consideration of the effect of I3C treatment in MDMs of three new SLE cases, DEGs of treated cases versus untreated cases (group 2) were investigated. The analysed data showed 758 upregulated and 285 downregulated genes. Among the upregulated genes, *TP53*, *MMP9*, *FN1*, *IL1B*, *MET*, *SRC*, *ETS1*, *CEACAM1*, *THBS1*, *CXCL5*, *TNIP3*, *TNFAIP6*, *EPPK1*, *CCR4*, *LAMA5*, *COL6A1*, *JUND*, *ANXA3*, *EGFL7*, *DMTN*, *USP11*, *PAK5*, *SYNPO*, *RHBDF2*, *FBRS*, *CD300E* and *CCM2L* were involved in the wound-healing process.

Comparison of DEGs in I3C-treated SLE cases and healthy controls

In order to investigate the effect of I3C on the gene expression profile of new SLE cases and healthy controls, a Venn diagram was generated. In a comparison of treated cases versus treated controls (group 3) using CLC Genomics Workbench, significant MDMs DE genes ($p \leq 0.05$) were identified. Among the overexpressed genes, *IL6*, *IL10*, *HGF*, *IL1B*, *IGF1*, *CXCL8*, *MET*, *TLR2*, *PLAU*, *HPSE*, *GJB2*, *F13A1*, *LTF*, *F2RL1*, *FOS*, *CD163*, *PRKCB*, *CASP1*, *SERPINB2*, *DYSF*, *CLEC7A*, *WNT7A*, *NOG*, *CLASP1*, *TNFSF10*, *CD14*, *TNFAIP3*, *F2R*, *ETS1*, *DPP4*, *THBS1*, *FCGR2A*, *FCGR3A*, *PTX3*, *EGR1*, *PRKCE*, *F13A1*, *F2RL1*, *FOS*, *CD163*, *PRKCB*, *CASP1*, *SERPINB2*, *DYSF*, *WNT7A*, *NOG*, *DST* and *CD300E* were involved in the wound-healing process.

SLE disease-related genes in the study group

To identify genes related to SLE disease, comparison of DEGs of untreated cases to untreated controls (group 4) was generated. The gene expression pattern of patients compared to controls revealed 818 upregulated and 588 downregulated genes. Among the overexpressed transcripts, *RP5-940J5.9*, *PKD1P1*, *RABGEF1-2*, *DCANP1*, *RP5-940J5.9*, *UPK3BL*, *RP11-707P17.1*, *NPIPA8*, *NPIPA7* and *CTC-510F12.6* were at the top of the list, with more than 200 fold changes. *RP11-949J7.8*, *RP11-324E6.6*, *RP11-514P8.8*, *RP5-850E9.3*, *AC002985.3*, *NUTM2E*, *CTD-2550O8.5*, *POU2AF1*, *TRAV26-1*, *TRBV27* and *BEGAIN* were downregulated, with more than 100 fold changes. Further analysis showed that *IL1B*, *LTF*, *F2RL1*, *TNFSF10*, *ETS1*, *THBS1* and *CD300E* were downregulated in untreated cases versus untreated controls (group 4), but interestingly, they were upregulated in treated cases versus treated controls (group 3).

Identification of co-DEGs by Venn diagram

The Venn diagrams of the upregulated and downregulated genes revealed significant DEGs (fold change >2 or <-2, $p<0.01$, paired *t*-test) in I3C-treated versus untreated cases, as well as between I3C-treated versus untreated controls. KEGG pathways mostly associated with the DEGs were obtained using Reactome.

Co-DEGs of new SLE cases and healthy controls post I3C treatment

The Venn diagram shows 327 overlapping genes between groups 1 and 2 (Figure1(a)). The identified genes were related to the effect of I3C on the gene expression profiles of new SLE cases and controls. Upregulation of 273 genes and downregulation of 54 genes were identified in I3C-treated groups versus untreated groups. Among the common upregulated genes, *F2RL2*, *FZD9*, *CDKN1A* and *FN1* were involved in the wound-healing process.

Co-DEGs of new SLE cases and healthy controls pre and post I3C treatment

The Venn diagram shows that among 394 overlapping genes between treated cases versus treated controls (group 3) and untreated cases versus untreated controls (group 4), 99 DEGs were upregulated in group 3 and downregulated in group 4 (Figure 1(b)). Among the overexpressed transcripts post I3C treatment, *IGHG2*, *C1S*, *C1R*, *IGKV1-5*, *IGKV4-1*, *SERPING1*, *IGKV3-11*, *STAT1*, *HDC*, *S1PR1*, *LCN2* and *NT5E* were involved in four stages of the wound-healing process.

Identification of hub co-DEGs involved in wound healing influenced by I3C

According to a comparison of groups 3 and 4, genes of a group that have a reverse expression pattern to the opposite group are I3C-affected genes. Genes that were downregulated in untreated groups and upregulated simultaneously in treated groups were significantly affected by I3C. The results revealed that among 394 co-DEGs, 358 genes were upregulated and 36 genes were downregulated in treated cases versus treated controls in comparison with untreated cases versus untreated controls. Among the major genes involved in the wound-healing process, *CD36*, *GAS6*, *DST*, *TREML1*, *P2RY1*, *ENPP4*, *TFPI*, *STXBP3*, *TLR4*, *PAPSS2*, *CD9*, *MERTK*, *ANXA1*, *BLOC1S6*, *HBEGF*, *SYT7*, *FN1* and *ALOX12* were upregulated. Among DEGs of groups 1–2 and 3–4, the network of 153 of common genes was generated as hub genes. DEG distributions of groups 1 and 2 by gene expression level are depicted as MA plots in Supplemental Figure S2(a) and (b). A PCA plot of all genes and genes involved in wound healing was constructed using the CLC Genomics Workbench. According to the PCA plots, untreated cases were positioned in a

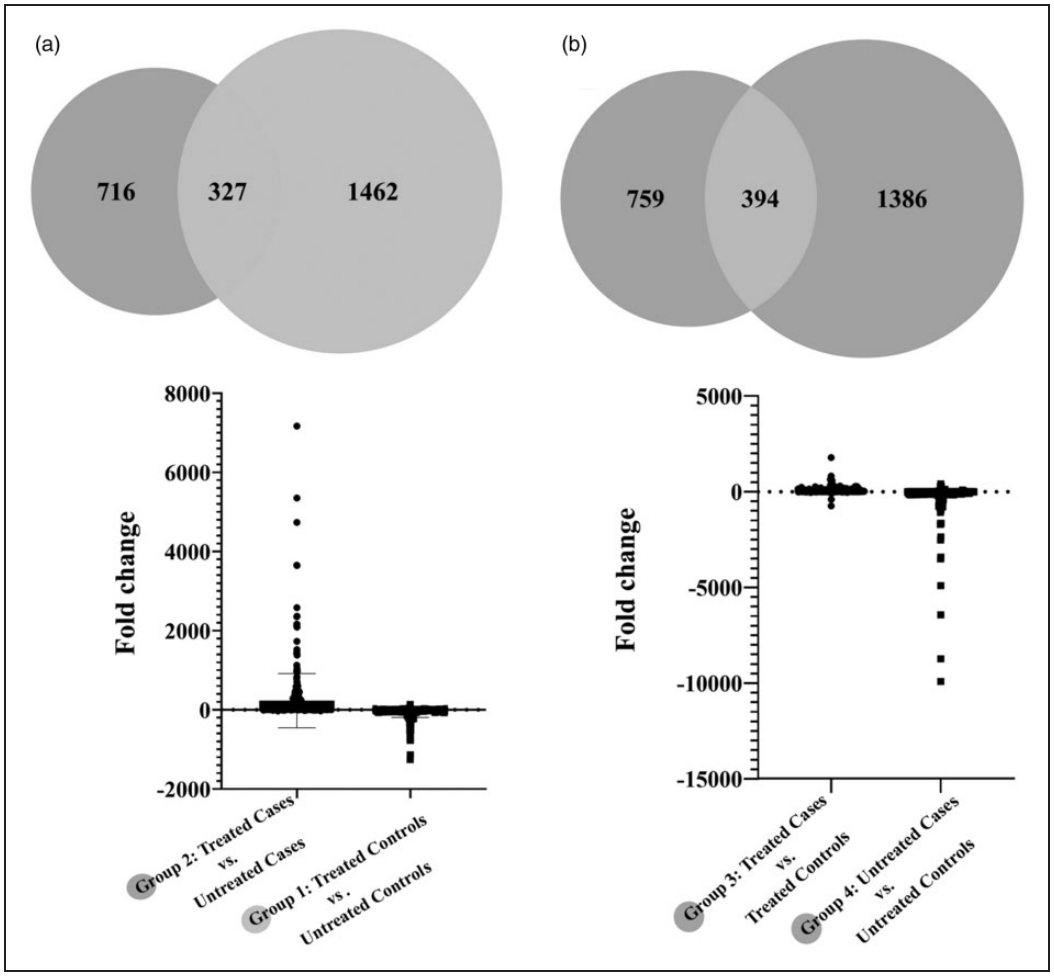

Figure 1. Representative Venn diagram of co-DEGs between groups 1 and 2 and groups 3 and 4. Common altered genes expressed with a valid *p*-value of ≤ 0.05 were identified in patients and controls post I3C treatment. (a) Incremental graph pattern of differential gene expression in I3C-treated cases versus treated controls. (b) Decreasing profile of gene expression in untreated cases and controls versus treated cases and controls. DEG: differentially expressed genes; I3C: indole-3-carbinol.

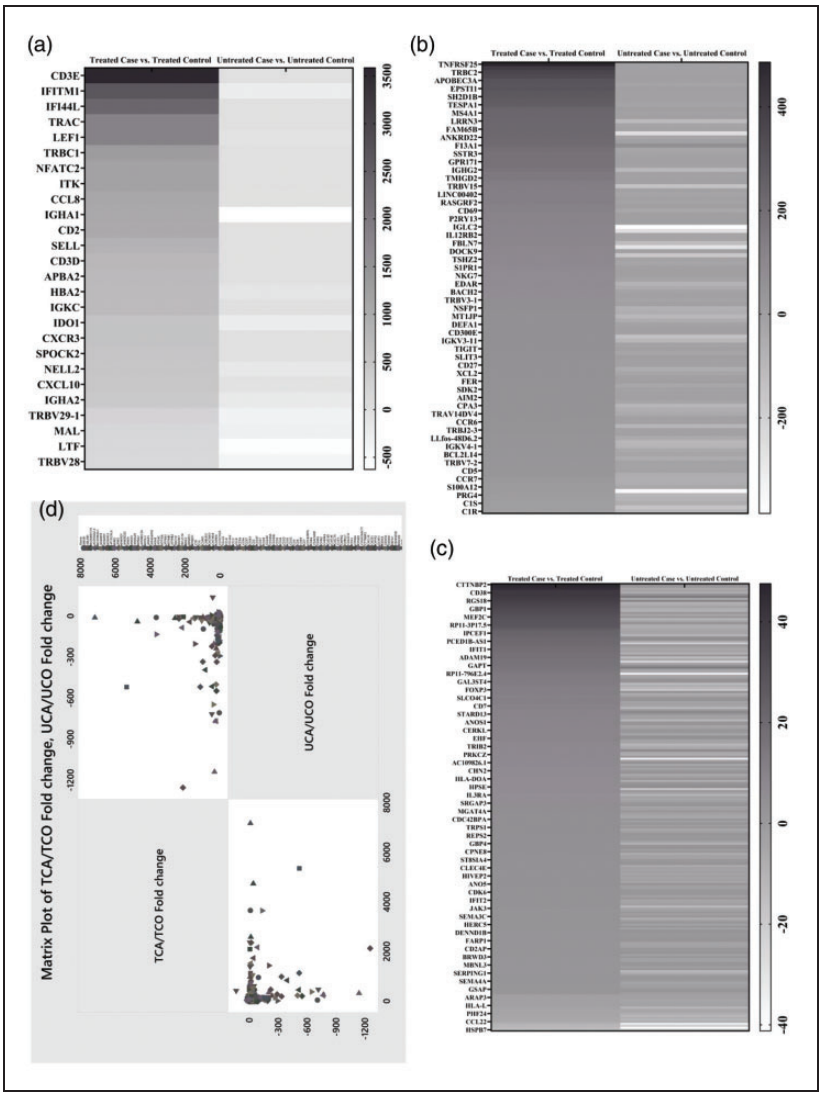

Figure 2. Heat map of RNA-seq data showing how the expression of MDM genes was affected by I3C treatment. For visualization of expression patterns of DEGs between new SLE cases ($n = 2$) and healthy controls ($n = 2$) post I3C treatment, heat maps were generated in purple and white scales using Minitab software. The columns indicate the patient's condition (case or control), while the rows reveal selected genes of group 3 with a criteria-adjusted p-value of ≤ 0.05 (Benjamini–Hochberg). RNA-seq: RNA sequencing; MDM: macrophage-derived monocytes; SLE: systemic lupus erythematosus.

distinct region (Supplemental Figure S3(a) and (b)). The position of the samples was changed post I3C treatment in the PCA plots.

Using a heat map, RPKM differential expression of genes from I3C-treated cases and untreated controls was evaluated. Gene enrichment of DEGs was determined by nominal $p \leq .05$ from the t-test for each gene in I3C-treated cases versus treated controls (group 3) and untreated cases versus untreated controls (group 4; Figure 2).

Validation of I3C effect on RNA-seq ranked genes

In the third phase of study, *CDKN1A*, *MMP15* and *FN1* – the genes involved in proliferative and remodelling stages of wound healing – were selected for qRT-PCR validation. The expression fold change of *CDKN1A* (5.96-fold), *MMP15* (5.61-fold) and *FN1* (1.63-fold) in qRT-PCR was compared to that of *CDKN1A* (4.37-fold), *MMP15* (5.6-fold) and *FN1* (7.12-fold) in treated cases versus untreated cases (group 2; Figure 3).

Discussion

MDMs play an important role in the wound-healing processes.[27] In earlier reports, we demonstrated that I3C plays a role in modulating the monocyte response.[22,28] In normal wound healing, macrophages first exhibit a pro-inflammatory M1 phenotype, and

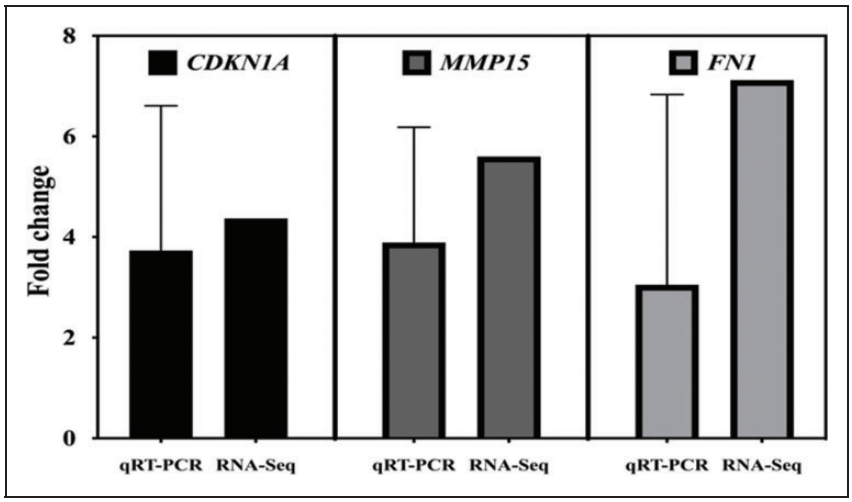

Figure 3. Validation of ranked genes by qRT-PCR for 15 new SLE cases. The expression levels of *CDKN1A*, *MMP15* and *FN1* were consistent with qRT-PCR results and were upregulated post I3C treatment. qRT-PCR: quantitative real-time polymerase chain reaction.

then switch to an alternatively activated M2 phenotype. To polarize M1 and M2 macrophages, several signalling molecules such as cytokines, Toll-like receptor agonists and growth factors are involved. True mimicking of the in vivo conditions for macrophage activation is critical to obtain unbiased results.[29] Thus, in order to reduce the effect of interfering factors in the MDM genes expression profile in SLE patients, autologous plasma was used in this study rather than M-CSF and GM-CSF synthetic growth factors to differentiate monocytes into macrophages.[30]

Among all the compared groups, group 2 was selected as the group that compared treated cases to untreated cases alone to discuss altered genes. AhR activation by I3C induction leads to upregulation of cytochrome P450 genes, including *IL-1β*, *CYP2J2*, *CYP27B1*, *POR*, *CYP2S1*, *FDXR*, *CYP2T1P* and *CYP4F11* in treated cases versus untreated cases (group 2).

In the haemostasis stage, among M1 macrophages, genes such as *JAK3*, *CCL8*, *STAT1*, *CCL5* and *FOXP3* that were involved in apoptosis, while *C1S*, *IL-1B*, *CXCL10* and *IL-12RB2*, which were implicated in the bacterial clearance procedure during the wound-healing process, were upregulated in groups 1 and 2. Scavenger receptor (SR) type I and type II genes such as macrophage scavenger receptor 1 (*MSR1*, *SR-AI* or *CD204*), macrophage collagenous structure receptor (*MARCO* or *SR-A6*) and *CD36* (SR-B2) that were highly expressed in M2 macrophages to control the balance of M1:M2 macrophages in the wound environment were identified among the DEGs of group 2.[31–33] *C1S*, *C1R*, *IGKV1-5*, *IGHV4-59*, *IGHV1-69*, *SEZ6L2*, *CLU*, *IGLV4-69*, *IGHG2*, *IGLV2-14*, *IGLV3-21*, *IGLV2-23*, *IGLV1-44*, *IGKV4-1*, *SERPING1*, *IGLC1*, *IGLC2*, *IGKV3-1* and *CFB* were upregulated, while the *MASP2* gene was downregulated in treated cases versus untreated cases (group 2).

In the inflammatory stage of wound healing, M2 macrophages produce IL-10 and stimulate epithelial cells plus fibroblasts by producing growth factors such as PDGF and TGFB1. In I3C-treated cases versus untreated cases (group 2), *ADAM19*, *CEACAM1*, *MMP17*, *COL10A1*, *ITGB7*, *THBS1*, *EMILIN1*, *CEACAM8*, *CAPN1*, *AGRN*, and *LRP10* were upregulated, while *DST* and *COL5A2* were downregulated. Furthermore, *CXCL10, CCL5* and *IL1B* were upregulated, while *COL5A2* was downregulated as the genes involved in IL-10 signalling in treated cases versus untreated cases (group 2).

The genes involved in extracellular matrix organization and immune complex resolution, including *LAMA5*, *COL6A1*, *FN1*, *MMP9*, *MMP15*, *THBS1* and *LIMS2*, were upregulated, while *FBN2*, *VCAM1*, *DST*, *ITGAD* and *COL5A2* were downregulated in treated cases versus untreated cases (group 2).[34]

Angiogenesis is a necessary part of proliferation, which is observed after four days of wound healing in response to the chemotactic material secreted from the platelets and macrophages.[35] *SRC*, *SPHK1*, *SCAP*, *PIK3R* and *BCAR1* were upregulated in I3C-treated cases versus untreated cases (group 2). *STAT1*, *SRC*, *COL6A1*, *PIK3R2*, *THBS1*, *ATP2A3* and *BCAR1* as the genes involved in PDGF signalling, along with those involved in growth hormone receptor signalling, including *SOCS3*, *SOCS1*, *STAT1* and *IRS1*, were upregulated, while *PRLR* was downregulated in treated versus untreated cases (group 2). Among

genes involved in the remodelling stage of wound healing *MEF2C*, *MYO1A* and *Arg1*[36–38] were significantly upregulated in I3C-treated cases versus untreated cases (group 2).

A limitation of this study is the small sample size. In order to obtain a more comprehensive understanding regarding the disparity of the immune-related genes in males and females, a larger number of subjects and utilization of integrated omics approaches would be necessary.

Conclusion

In summary, regarding the results obtained via RNA-seq, all patients had almost the same expression pattern before I3C treatment, but their expression pattern changed after treatment, which may be related to SLE personalized differences. Expression levels of genes involved in wound healing through activating PI3K/Akt and ERK/MAPK pathways were elevated. Furthermore, an increase in the expression of anti-inflammatory macrophages represented promotion of M2 macrophage polarization. Thus, it seems that I3C can be used to improve wound healing in SLE patients.

Acknowledgements

We thank all the investigators who contribute to the SLE field.

Declaration of competing of interest

The authors declared no potential conflicts of interest with respect to the research, authorship and/or publication of this article.

Funding

The authors disclosed receipt of the following financial support for the research, authorship and/or publication of this article: This article was derived from a thesis of a PhD degree in the field of Molecular Medicine at School of Advanced Technologies in Golestan University of Medical Sciences, Gorgan, Iran (Grant Number: 951126263).

ORCID iDs

Farnaz Eghbalpour https://orcid.org/0000-0002-6569-2656
Saeed Mohammadi https://orcid.org/0000-0001-9895-8468
Yaghoub Yazdani https://orcid.org/0000-0003-4005-3521

Supplemental material

Supplemental material for this article is available online.

References

1. Krzyszczyk P, Schloss R, Palmer A, Berthiaume F. The role of macrophages in acute and chronic wound healing and interventions to promote pro-wound healing phenotypes. *Front Physiol* 2018; 9: 419.
2. Orme J, Mohan C. Macrophage subpopulations in systemic lupus erythematosus. *Discov Med* 2012; 13: 151–158.
3. Bosurgi L, Cao YG, Cabeza-Cabrerizo M, et al. Macrophage function in tissue repair and remodeling requires IL-4 or IL-13 with apoptotic cells. *Science* 2017; 356: 1072–1076.
4. Zhu C, Xie Q, Zhao B. The role of AhR in autoimmune regulation and its potential as a therapeutic target against CD4 T cell mediated inflammatory disorder. *Int J Mol Sci* 2014; 15: 10116–10135.
5. Burke CG, Boule LA, Lawrence BP, Fenton BM, Thevenet-Morrison K, Jusko TA. Developmental activation of the AHR increases effector CD4+ T cells and exacerbates symptoms in autoimmune disease-prone Gnaq+/− mice. *Toxicol Sci* 2015; 148: 555–566.
6. Goudot C, Coillard A, Villani AC, et al. Aryl hydrocarbon receptor controls monocyte differentiation into dendritic cells versus macrophages. *Immunity* 2017; 47: 582–596.e6.
7. Yazdani Y, Keyhanvar N, Kalhor HR, Rezaei A. Functional analyses of recombinant mouse hepcidin-1 in cell culture and animal model. *Biotechnol Lett* 2013; 35: 1191–1197.
8. Roohi A, Yazdani Y, Khoshnoodi J, et al. Differential reactivity of mouse monoclonal anti-HBs antibodies with recombinant mutant HBs antigens. *World J Gastroenterol* 2006; 12: 5368–5374.
9. Beischlag TV, Luis Morales J, Hollingshead BD, Perdew GH. The aryl hydrocarbon receptor complex and the control of gene expression. *Crit Rev Eukaryot Gene Expr* 2008; 18: 207–250.
10. Larigot L, Juricek L, Dairou J, Coumoul X. AhR signaling pathways and regulatory functions. *Biochim Open* 2018; 7: 1–9.
11. Ohtake F, Takeyama K, Matsumoto T, et al. Modulation of oestrogen receptor signalling by association with the activated dioxin receptor. *Nature* 2003; 423: 545–550.
12. Beischlag TV, Luis Morales J, Hollingshead BD, Perdew GH. The aryl hydrocarbon receptor complex and the control of gene expression. *Crit Rev Eukaryot Gene Expr* 2008; 18: 207–250.
13. Nagafuchi Y, Shoda H, Fujio K. Immune profiling and precision medicine in systemic lupus erythematosus. *Cells* 2019; 8: 140.
14. Jiang J, Kang TB, Shim do W, Oh NH, Kim TJ, Lee KH. Indole-3-carbinol inhibits LPS-induced inflammatory response by blocking TRIF-dependent signaling pathway in macrophages. *Food Chem Toxicol* 2013; 57: 256–261.
15. Tsai JT, Liu HC, Chen YH. Suppression of inflammatory mediators by cruciferous vegetable-derived indole-3-carbinol and phenylethyl isothiocyanate in lipopolysaccharide-activated macrophages. *Mediators Inflamm* 2010; 2010: 293642.
16. Tsuji N, Fukuda K, Nagata Y, et al. The activation mechanism of the aryl hydrocarbon receptor (AhR) by

molecular chaperone HSP90. *FEBS Open Bio* 2014; 4: 796–803.
17. Sarr EHM, Mayrand M-H, Coutlée F, et al. Exploration of the effect of human papillomavirus (HPV) vaccination in a cohort of pregnant women in Montreal, 2010–2016. *Heliyon* 2019; 5: e02150.
18. Gladman DD, Ibañez D, Urowitz MB. Systemic Lupus Erythematosus Disease Activity Index 2000. *J Rheumatol* 2002; 29: 288–291.
19. Conesa A, Madrigal P, Tarazona S, et al. A survey of best practices for RNA-seq data analysis. *Genome Biol* 2016; 17: 13.
20. Frykberg RG, Banks J. Challenges in the treatment of chronic wounds. *Adv Wound Care* 2015; 4: 560–582.
21. Bhattacharjee J, Das B, Mishra A, Sahay P, Upadhyay P. Monocytes isolated by positive and negative magnetic sorting techniques show different molecular characteristics and immunophenotypic behaviour. *F1000Res* 2017; 6: 2045.
22. Mohammadi S, Memarian A, Sedighi S, Behnampour N, Yazdani Y. Immunoregulatory effects of indole-3-carbinol on monocyte-derived macrophages in systemic lupus erythematosus: a crucial role for aryl hydrocarbon receptor. *Autoimmunity* 2018; 51: 199–209.
23. Wickramasinghe S, Rincon G, Islas-Trejo A, Medrano JF. Transcriptional profiling of bovine milk using RNA sequencing. *BMC Genom* 2012; 13: 45.
24. Fabregat A, Sidiropoulos K, Viteri G, et al. Reactome pathway analysis: a high-performance in-memory approach. *BMC Bioinformatics* 2017; 18: 142.
25. Yamaguchi M, Hankinson O. 2,3,7,8-tetrachlorodibenzo-p-dioxin suppresses the growth of human colorectal cancer cells in vitro: implication of the aryl hydrocarbon receptor signaling. *Int J Oncol* 2019; 54: 1422–1432.
26. Eghbalpour F. *MDMs RNA-Seq*. V1 ed. Harvard Dataverse, 2020.
27. Kim SY, Nair MG. Macrophages in wound healing: activation and plasticity. *Immunol Cell Biol* 2019; 97: 258–267.
28. Mohammadi S, Seyedhosseini FS, Behnampour N, Yazdani Y. Indole-3-carbinol induces G1 cell cycle arrest and apoptosis through aryl hydrocarbon receptor in THP-1 monocytic cell line. *J Recept Signal Transduct Res* 2017; 37: 506–514.
29. Wang N, Liang H, Zen K. Molecular mechanisms that influence the macrophage m1–m2 polarization balance. *Front Immunol* 2014; 5: 614.
30. Araki H, Katayama N, Mitani H, et al. Efficient ex vivo generation of dendritic cells from CD14+ blood monocytes in the presence of human serum albumin for use in clinical vaccine trials. *Br J Haematol* 2001; 114: 681–689.
31. Poon IK, Lucas CD, Rossi AG, Ravichandran KS. Apoptotic cell clearance: basic biology and therapeutic potential. *Nat Rev Immunol* 2014; 14: 166–180.
32. Zani IA, Stephen SL, Mughal NA, et al. Scavenger receptor structure and function in health and disease. *Cells* 2015; 4: 178–201.
33. Wermeling F, Chen Y, Pikkarainen T, et al. Class A scavenger receptors regulate tolerance against apoptotic cells, and autoantibodies against these receptors are predictive of systemic lupus. *J Exp Med* 2007; 204: 2259.
34. Ugarte-Berzal E, Boon L, Martens E, et al. MMP-9/gelatinase B degrades immune complexes in systemic lupus erythematosus. *Front Immunol* 2019; 10.
35. Ucuzian AA, Gassman AA, East AT, Greisler HP. Molecular mediators of angiogenesis. *J Burn Care Res* 2010; 31: 158–175.
36. Murray PJ, Allen JE, Biswas SK, et al. Macrophage activation and polarization: nomenclature and experimental guidelines. *Immunity* 2014; 41: 14–20.
37. Filomena MC, Bang M-L. In the heart of the MEF2 transcription network: novel downstream effectors as potential targets for the treatment of cardiovascular disease. *Cardiovasc Res* 2018; 114: 1425–1427.
38. Du C, Weng Y, Lou J, et al. Isobaric tags for relative and absolute quantitation-based proteomics reveals potential novel biomarkers for the early diagnosis of acute myocardial infarction within 3 h. *Int J Mol Med* 2019; 43: 1991–2004.